NEW CALCULATION SOFTWARE FOR ANALYTIC SUPPORT STRUCTURE OPTIMIZATION IN METAL ADDITIVE MANUFACTURING

Tiefnig Raphael, Haas Franz – Graz University of Technology, Austria

ABSTRACT

Powder based additive manufacturing systems often require support structures for overhanging geometries and thermal dissipation. On the one hand, the support material should be reduced to a minimum. On the other hand, the stiffness of the structures can be used as a fixture for post-processing. The contribution presents a unique analytic model to determine the stresses occurring in the support structures during post-processing. FEM simulations with different support types are carried out to validate the new calculation model. The results of this analysis subsequently serve as basis for dimensioning the support elements of complex and large parts. By specifying a machining process, it is possible to determine the required dimensions of the support structure (e.g. block, rod or cross). The aim of this optimization process is to reduce machining time, material consumption and post-processing costs. The results of the paper and the new software help to implement direct machining into industrial 3D printing processes.

KEYWORDS

Additive manufacturing, Selective Laser Melting, support structures, support optimization, post-processing, Direct Machining (DM)

INTRODUCTION

Additive manufacturing processes offer many possible applications, especially for industrial uses, due to their almost limitless design possibilities. Many processes [1], such as selective laser melting (SLM), selective laser sintering (SLS), electron beam melting (EBM) or 3D printing, have already found their way into industrial manufacturing. Nowadays, additive manufacturing is no longer limited to prototyping, metal additive manufacturing in particular enables the production of finished parts in small batches [2]. Additive processes offer several advantages over conventional processes such as milling or turning. The production of lattice or lightweight structures is possible, thus topology-optimized components can be manufactured. Functional integration of assemblies can be realized. Holes, channels and cooling elements can be implemented directly in the printing process [3].

However, the manufacturing concept of the layer-by-layer structure of additive manufacturing also entails limitations. With most processes, the use of support structures [4] is required when building up geometries with an overhang angle of more than 45 degrees. The support structure also helps to prevent cracking, compensate deformations due to high residual stresses and facilitate heat dissipation, since loose powder has very poor thermal conductivity [5]. These support elements have to be removed from the component during post-processing. In general, the rough surface finish of additively manufactured parts usually requires post-processing [6]. This applies in particular to functional surfaces, fits, but also holes and threads usually have to be reworked. Since the components are connected to the build plate via the support structures and therefore form a rigid clamping of the parts on the build plate. These support structures can be used as clamping of the components for the machining post-processing. This machining concept has been established and researched at the IFT [7] and can be described by the term "Direct Machining". This refers to the post-processing of SLM

parts, which are connected to the building plate via the support structure. In this way, several parts can be reworked at the same time, which brings economic advantages because the parts do not have to be detached from the build plate beforehand and then reworked individually.

For DM [7], the prerequisite is that the support structures are designed in such a way that they can absorb the forces occurring during post-processing. The aim of the support structure is to give the component as much stability as possible while keeping the required volume of support elements to a minimum, because the additional support structure increases the overall build time and the support material is waste and has to be disposed [8]. For the optimum design of the support geometry, it is important to know the loads that occur during post-processing. This requires knowledge of the component geometry and information on the post-processing activity (milling, drilling, etc.). Based on this, a new developed calculation model determines the ideal parameters of the respective support structure for the following direct machining.

1. THEORETICAL STRESS MODEL

The theoretical load model described here is initially limited to the investigation of normal stresses, such as those that occur during face milling.

1.1 CUTTING FORCE DURING FACE MILLING

The process is used to create planar surfaces, so it is possible to compensate deviations in terms of dimensional and shape tolerance that occurred during the printing process [6]. In addition, this processing also serves to create surfaces with a significantly better surface quality than it is possible through layer-by-layer buildup in the SLM, SLS or EBM processes.

The cutting force [9] results from the chip cross-section A and the specific cutting force, whereby the specific cutting force $k_{c1.1}$ refers to a chip cross-section of 1 mm^2.

$$A = a_p * f = b * h \tag{1}$$

$$F_c = k_{c1.1} * b * h = k_{c1.1} * a_p * f_z \tag{2}$$

Equation 2 gives the cutting force on a single cutting edge in maximum intervention. To calculate the average cutting force on a cutting edge, the average chip thickness h_m is defined in the literature [8] by an approximation:

$$h_m = f_z * \sin \varphi * \sin \kappa \tag{3}$$

Figure 1 shows the meshing ratios for symmetrical face milling and on the right side the cutting force curve along the contact angle φ.
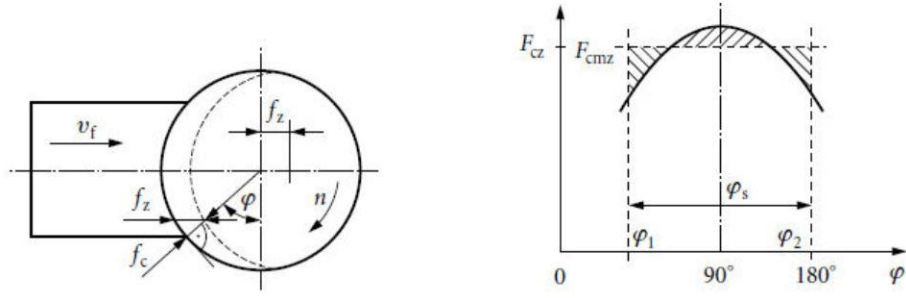
Fig. 1: Cutting conditions for symmetric face milling

Assuming symmetrical machining, the following formulas for the average cutting force result, according to Degner [10]:

$$F_{cm} = \frac{180°}{\varphi_s * \pi} * \int_{\varphi_1}^{\varphi_2} F_c * d_\varphi \tag{4}$$

$$F_{cm} = \frac{180°}{\varphi_s * \pi} * k_c * b * f_z * \sin \kappa * \frac{2 * a_e}{D} \tag{5}$$

Equation 5 includes the chip width b, the cutting arc angle φ_s, the specific cutting force k_c, the feed per tooth f_z, the setting angle κ, the operational reach a_e and the tool diameter D.

1.3 SUPPORT STRUCTURES

Three different support variants [8] were used for the calculation model. Figure 2 shows the geometries of these support elements.
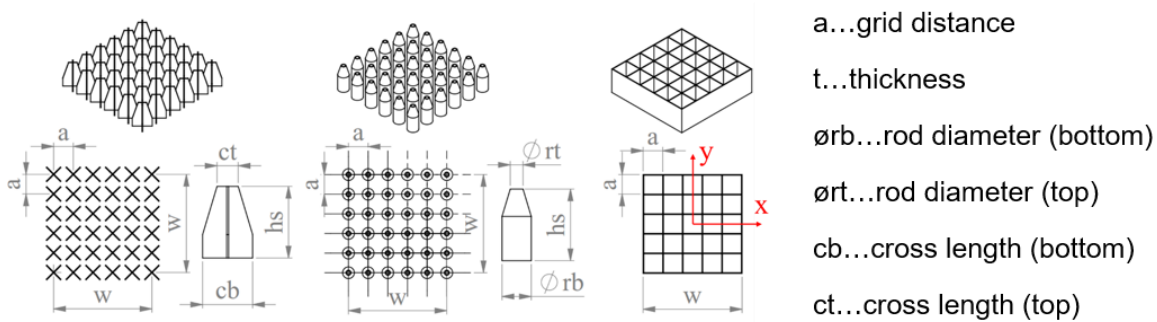

a…grid distance

t…thickness

ørb…rod diameter (bottom)

ørt…rod diameter (top)

cb…cross length (bottom)

ct…cross length (top)

Fig. 2: Support elements, Cross-Support (left), Rod-Support (middle) & Block-Support (right) [8]

In all three cases, the geometry of a single support element is used to determine the cross-sectional properties. The most important properties, in relation to the strength calculation, are the geometrical moment of inertia I_x and the section modulus W_x. The calculation is limited to the determination of the axial section modulus, which is required later for the determination of the bending stress. Another important property is the cross-sectional area, because from this the volume and thus the material consumption of the support structure can be derived. The starting point for the calculation of the geometrical moment of inertia of the structure is the geometrical moment of inertia of a single support element. The following relationships result for the three variants:

$$I_{x,block} = \frac{a_x * a_y^3}{12} - \frac{(a_x - t) * (a_y - t)^3}{12} \tag{6}$$

$$I_{x,rod} = \frac{\pi}{64} * (d_{rod}{}^4 - (d_{rod} - 2 * t)^4) \tag{7}$$

$$I_{x,cross} = (l_{cross}{}^3 + (l_{cross} - t) * t^2) * \frac{t}{12} \tag{8}$$

Steiner's theorem then adds up the individual elements to the total cross section of the support structure. The formula for this is:

$$I_x = \sum_{i=1}^{n_{sx}*n_{sy}} (I_{x,i} + A_i * y_{ca}{}^2) \tag{9}$$

Equation 9 describes the geometrical moment of inertia of the entire support structure with I_x, the geometrical moment of inertia of a support element with $I_{x,i}$ and its cross-sectional area with A_i. The distance between the centroid of an element and the overall centroid is defined as y_{ca}. The number of support elements in x- and y-direction is given by n_{sx} and n_{sy}. From the previously determined geometrical moment of inertia, the section modulus can be calculated by knowing the edge fiber spacing $e_{x,y}$, which is subsequently used to calculate the bending stress.

$$W_x = \frac{I_x}{e_y} \quad \text{or} \quad W_y = \frac{I_y}{e_x} \tag{10}$$

The cross-sectional area of the entire support structure can also be calculated based on the cross-section of a single support element. The individual areas are simply added up later to give the total cross-sectional area of the support structure. Another important value is the support volume, which is determined with the help of the cross-sectional area and the corresponding support height h_s.

Table 1: Various support configurations [8]

	Filling level		
	W	M	S
General			
Grid pattern	6x6	8x8	10x10
Grid distance a (in mm)	2,74	1,96	1,52
Grid thickness t (in µm)	100	100	100
Support height hs (in mm)	4	4	4
Total grid width w (in mm)	13.7	13.7	13.7
Block Support			
Volume V_B	64.80	85.76	106.4
$I_{x,y}$ top (in mm⁴)	304.84	384.35	463.69
Rod Support			
Volume V_R (in mm³)	61.26	80.54	98.95
Rod diameter top Ørt (in mm)	0.71	0.54	0.44
Rod diameter bottom Ørb (in mm)	1.63	1.19	0.94
$I_{x,y}$ top (in mm⁴)	151.43	177.99	204.10
$I_{x,y}$ bottom (in mm⁴)	383.99	444.00	506.82
Cross Support			
Volume V_C (in mm³)	63.32	85.22	106.81
Cross length top ct (in mm)	1.18	0.85	0.68
Cross length bottom cb (in mm)	2.79	1.98	1.54
Ix,y top (in mm⁴)	178.63	206.28	241.03
Ix,y bottom (in mm⁴)	438.51	500.94	572.71

Table 1 shows the cross-sectional properties of the support structures [8] ("Block", "Rod", "Cross") for three different configurations ("W", "M", "S").

1.2 NOTCH EFFECT

The stress distribution depends not only on the external load and on the type of stress, but also very much on the cross-sectional changes (transitions, recesses, holes, grooves, etc.) [11]. Particularly at the transition between the building plate and the support structure as well as at the transition between the component and the support structure, discontinuous cross-sectional changes take place. Increased notch effects occur at these transitions, resulting in an increase in stress. This notch effect must be taken into account when optimizing or designing the support structures. FEM analyses are used to investigate different configurations of the support elements with regard to the notch effect that occurs. A very simple way to characterize the notch effect is by using the notch factor α_σ, which is defined by the ratio of the stress peak σ_{max} to the nominal stress σ_N [11]. The results of the analyses serve as the basis for defining approximation curves for the notch effect for the three support variants. These approximation curves are used to take the notch effect into account when designing the support parameters in the calculation model.
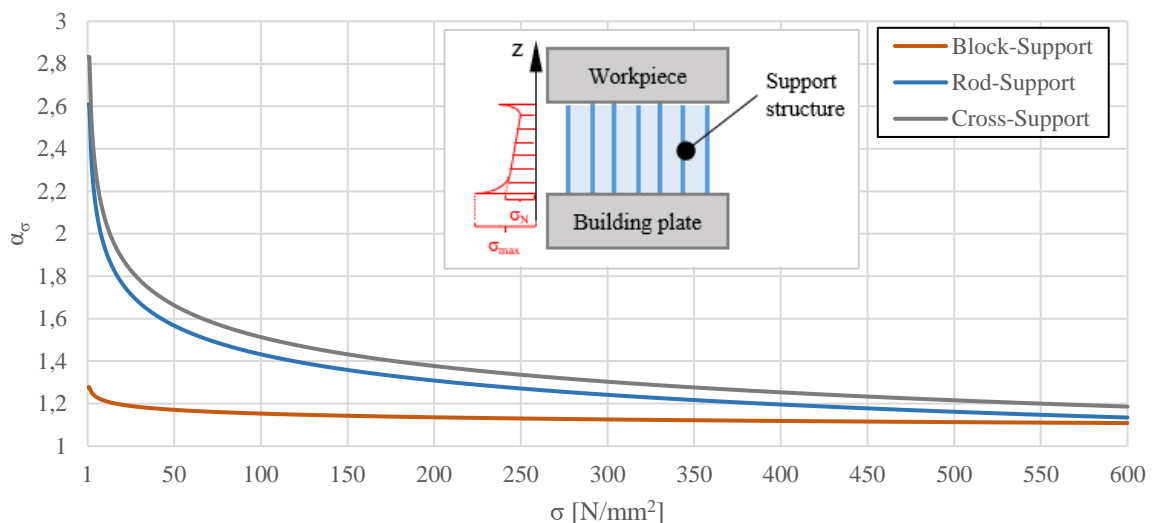

Fig. 3: Approximation curves for notch shape factor as a function of the occurring normal stress

The figure 3 shows the curves of the notch coefficients α_σ as a function of the occurring normal stress. FEM analyses of different support configurations form the basis for these three approximation curves derived for block, rod and cross support. The analyses show that the influence of the notch effect is smallest for the block support and the largest notch coefficients occur for the cross support. The influence of the notch effect decreases with increasing normal stress for all structures.

2. OPTIMIZATION PROCESS

The optimization process of the software works based on the previously described theoretical calculations. Depending on the user's specifications, the software runs through different program steps. The input mask of the program contains mandatory fields (e.g. workpiece geometry, material specifications and support variant) which are always necessary for the calculation. Further inputs

regarding the support geometries or the specification of a post-processing process influence the program run.

If the user does not specify any post-processing, then the software cannot optimize the support structure and the user must specify the support structure parameters himself. The program calculates the cross-section properties and the support volume using the specifications based on the theoretical calculation model. If information about a post-processing activity is available, then the software model can determine the required parameters of the support structures itself. The user has the possibility to control or limit the degree of optimization by entering his own data in the support parameters. Once the calculation process is complete, the results are displayed in an output window. In the software model, the optimization process takes place while passing through several loops. The user specifies the load occurring in the component or support structure by specifying the machining process. From this, the software can determine the required cross-sectional properties of the support elements. In the program loops, the variable support parameters are adjusted until the required values are reached. Figure 4 shows schematically the program flow for the optimization of a support structure of the type Rod-Support. In this example, the parameters grid spacing, thickness and diameter are varied during the loop pass until the required cross-section properties are achieved. The boundary conditions for the run variables are defined by specifications such as the component geometry or support geometry. If the requirements are met, the software saves the parameter configuration. When several parameters meet the requirements, the software selects the best variant. One selection criterion for this is, for example, a minimum cross-sectional area or a minimum support volume.
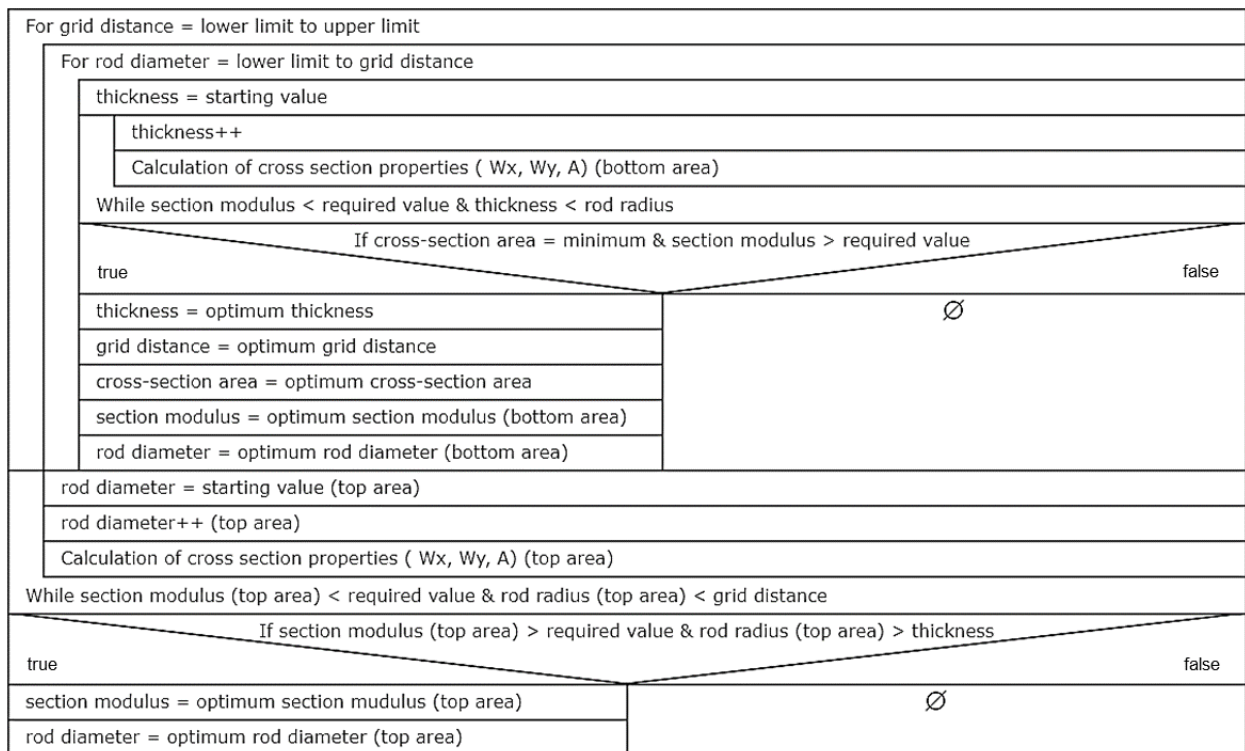
For grid distance = lower limit to upper limit
For rod diameter = lower limit to grid distance
thickness = starting value
thickness++
Calculation of cross section properties (Wx, Wy, A) (bottom area)
While section modulus < required value & thickness < rod radius
If cross-section area = minimum & section modulus > required value
true / false
thickness = optimum thickness / ∅
grid distance = optimum grid distance
cross-section area = optimum cross-section area
section modulus = optimum section modulus (bottom area)
rod diameter = optimum rod diameter (bottom area)
rod diameter = starting value (top area)
rod diameter++ (top area)
Calculation of cross section properties (Wx, Wy, A) (top area)
While section modulus (top area) < required value & rod radius (top area) < grid distance
If section modulus (top area) > required value & rod radius (top area) > thickness
true / false
section modulus = optimum section mudulus (top area) / ∅
rod diameter = optimum rod diameter (top area)

Fig. 4: Loop pass during the optimization process of a rod support structure

Depending on the selected support type, there are different parameters that can be adjusted by the optimization model to achieve the required strength properties. Table 2 shows the variable parameters for the three different support structures.

Table 2: Optimization parameters for the selected support structures (block, rod, cross)

	Block	Rod	Cross
Grid distance	✓	✓	✓
Thickness	✓	✓	✓
Support dimension (top area)		✓	✓
Support dimension (bottom area)		✓	✓

3. VERIFICATION OF THE CALCULATION MODEL

In order to verify the suitability of the calculation model, practical machining tests [8] are carried out. The tests are performed on a 5-axis milling machine and the cutting forces are measured using a Kistler Multicomponent Dynamometer (type 9129AA) in combination with a Kistler 5070A10100 charge amplifier. A 25 mm diameter face milling cutter with one cutting edge is used for face milling [8]. The cutting depth in the tests is between 0.1 mm and 1.5 mm. The parameters for the cutting force calculation can be taken from Table 3.

Table 3: Cutting parameters for the milling tests

Milling cutter diameter D	25 mm
Number of cutting edges	1
Specific cutting force $k_{c1.1}$	2550 N/mm² (316L)
Setting angle κ	85°
Feed per tooth f_z	0,05 mm
Cutting depth a_p	0.1 – 1.5 mm
Milling width a_e	14 mm
Material constant m_c	0.18

The support parameters (W, M, S) as shown in Table 1 are used as test structures [8]. The support height is 4 mm and the test components have a square cross-section (14 mm x 14 mm). Table 4 shows the theoretical cutting forces, based on the previously described calculation schema, at different cutting depths a_p.

Table 4: Theoretical cutting force F_c at different cutting depths a_p

a_p [mm]	0.1	0.25	0.5	1	1.5
F_c [N]	20.8	51.1	104.2	208.3	312.5

Figure 5 shows the measured cutting forces at different cutting depths. When machining the rod support, the support structure fails at the configuration "W" of a cutting depth a_p of 1 mm. The cross support (configuration "W") already fails at a cutting depth of 0.5 mm.

Figure 6 shows the comparison between the measured cutting force from the cutting tests and the calculated theoretical cutting force. The curves show the calculated cutting force matches the measured values very well.
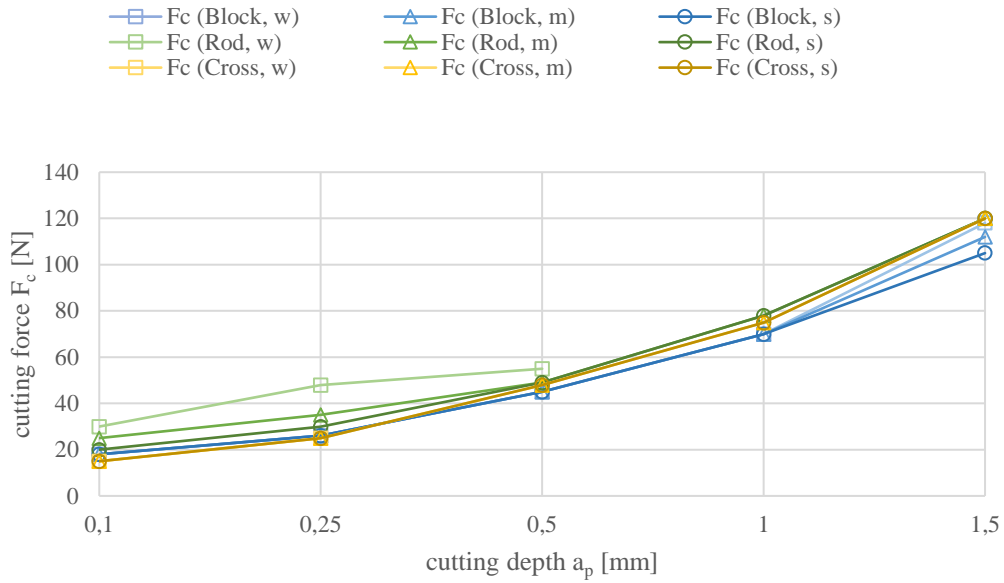
Fig. 5: Measured cutting forces for the different support structures
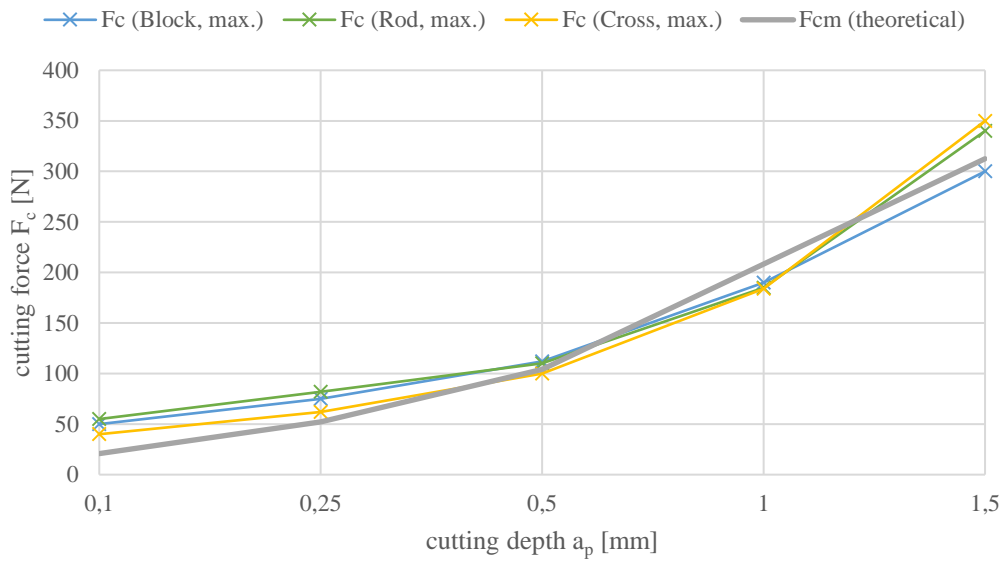

Fig. 6: Theoretical cutting force curve compared to maximum measured cutting forces

The results from the machining tests show that the selected support configurations are not ideally designed for the corresponding machining. With the help of the developed calculation model, the parameters of the support structures are optimized. Table 5 shows the results of the optimization for the rod support structure. The fields marked in green are the parameters that are available to the program for optimization.

Table 5: Example of a support structure optimization for a given finishing operation (face milling)

Dimensions in mm	Rod support „W"					Rod support „optimized"				
Support height	4					4				
Grid distance	2.74					2.74	2.74	2.74	2.74	2.7
Thickness	0.1					0.1	0.1	0.1	0.34	0.47
Rod diameter (top)	0.71					0.24	0.44	0.79	0.74	0.95
Rod diameter (bottom)	1.63					0.27	0.53	0.98	0.85	1.04
W_{XY} (top)	21.013					4.975	11.918	23.651	46.722	75.287
W_{XY} (bottom)	50.097					6.029	14.984	29.824	59.154	88.899
a_p [mm]	0.1	0.25	0.5	1	1.5	0,1	0,25	0,5	1	1,5
F_c [N]	20.8	52.08	104.17	208.34	312.60	20.80	52.08	104.17	208.34	312.6
σ_z [N/mm^2]	14.85	37.18	73.36	148.72	223.15	62.71	65.55	66.07	66.89	62.28
σ_z [N/mm^2]	7.89	19.75	39.51	79.02	118.56	65.55	66.04	66.36	66.92	66.81
Machining test passed	✓	✓	✓			✓	✓	✓	✓	✓

The optimization software selects the support parameters so that the structures can withstand the loads that occur. The findings from the machining tests [8] performed are used for the dimensioning.

4. CONCLUSION

In its current form, the optimization software forms a rough model for support structure design in combination with direct machining. Optimization of the support structure offers several advantages, such as shortening the build time, reducing powder consumption and optimizing post-processing. The goal is to implement the optimization software in existing AM programs, in order to integrate the Direct Machining process already during job preparation. The calculation model represents a first prototype. However, there are still some development steps necessary to be able to integrate the software into industrial applications. In particular, the creation of the load model for various reworking processes requires further development work.

Nevertheless, the optimization model of support structures has great potential in the field of additive manufacturing and can contribute to improvements in post processing, but also to the optimization of the actual manufacturing process.
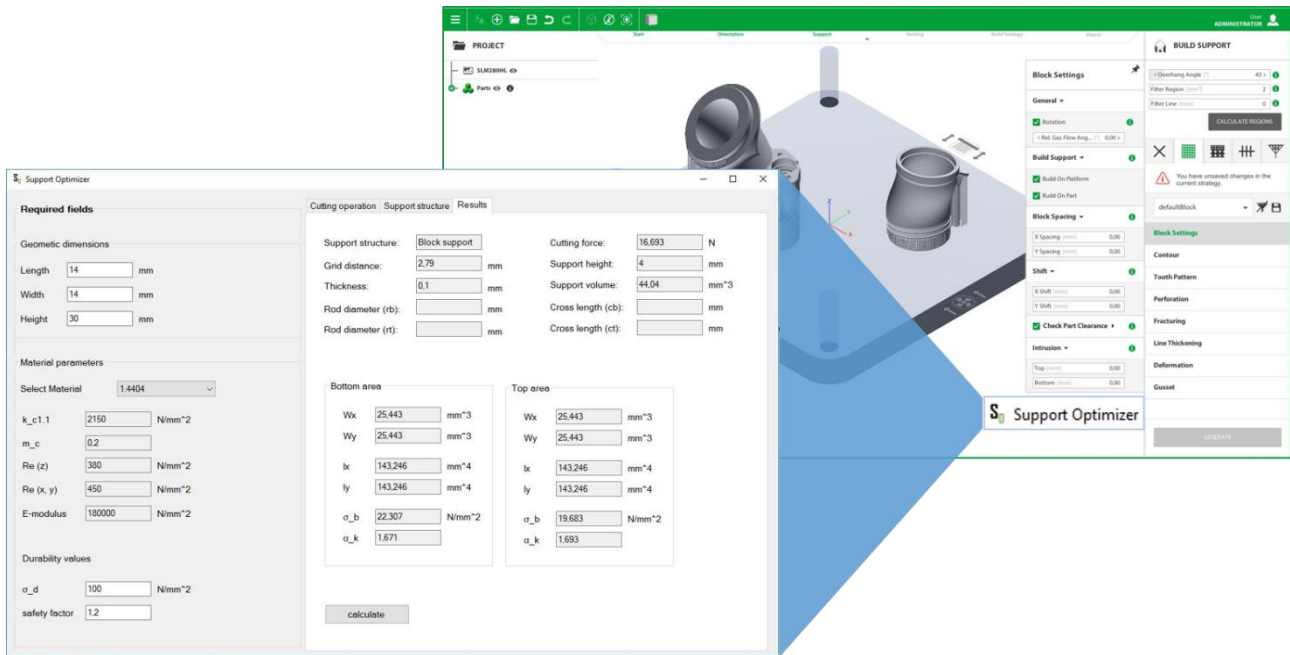
Fig. 7: Input window and possible implementation of the "Support Optimizer" optimization software

REFERENCES

[1] J. ILG, Systematische Eignungsanalyse zum Einsatz additiver Fertigungsverfahren. Springer Gabler Verlag, Wiesbaden (2019), p. 5 – 15.

[2] R. LACHMAYER, R. B. LIPPERT, 3D-Druck beleuchtet: Additive Manufacturing auf dem Weg in die Anwendung. Springer Verlag, Berlin Heidelberg (2016), p. 1 – 3.

[3] F. KLOCKE, Fertigungsverfahren 5: Gießen, Pulvermetallurgie, Additive Manufacturing, Springer-Vieweg Verlag (2015), p. 163.

[4] D. I. WIMPENNY, P. M. PANDEY, L. J. KUMAR, Advances in 3D Printing & Additive Manufacturing Technologies, Springer, Singapore (2017), p. 15.

[5] T. MISHUROVA, S. CABEZA, T. THIEDE, ET AL., The Influence of the Support Structure on Residual Stress and Distortion in SLM Inconel 718 Parts. Metall Mater Trans A 49 (2018), p. 3038–3046.

[6] I. GIBSON, D. ROSEN, B. STUCKER, Additive Manufacturing Technologies: 3D Printing, Rapid Prototyping and Direct Digital Manufacturing. Springer Verlag, New York (2015), p. 329 - 350.

[7] C. HÖLLER, T. HINTERBUCHNER, P. SCHWEMBERGER, P. ZOPF, R. PICHLER, F. HAAS, Direct Machining of selective laser melted components with optimized support structures. Procedia CIRP Vol. 81 (2019), p. 375 - 380.

[8] C. HÖLLER, P. ZOPF, P. SCHWEMBERGER, R. PICHLER, F. HAAS, Load capacity of support structures for Direct Machining of selective laser melted parts. ASME 2019, Salt Lake City (2019), DOI 10.1115/IMECE2019-11134.

[9] J. DILLINGER, Fachkunde Metall – Mechanische Technologie. Europa-Lehrmittel, Haan-Gruiten (2010), p. 149.

[10] W. DEGNER, H. LUTZE, E. SMEJKAL, Spanende Formung. Carl Hanser Verlag, Berlin (2015), p. 167 – 208.

[11] H. WITTEL, D. MUHS, D. JANNASCH, J. VOßIEK, Roloff/Matek Maschinenelemente. Vieweg+Teubner, Wiesbaden (2011), p. 52-55.